TRPM7, Calcium and the cytoskeleton

Langeslag, Michiel

Chapter II

Gq/Phospholipase C-coupled agonists activate TRPM7 channels under physiological conditions

Michiel Langeslag, Kristopher Clark, Wouter H. Moolenaar, Frank N. van Leeuwen, Kees Jalink

Submitted to The Journal of Biological Chemistry

Gq/Phospholipase C-coupled Agonists Activate TRPM7 Channels under Physiological Conditions

Michiel Langeslag[*], Kristopher Clark[§], Wouter H. Moolenaar[#], Frank N. van Leeuwen[§,#], Kees Jalink[*]

[*] Division of Cell Biology, and
[#] Division of Cellular Biochemistry, the Netherlands Cancer Institute
Plesmanlaan 121, 1066 CX Amsterdam, the Netherlands, and
[§] Department of Tumor Immunology,
Nijmegen Centre for Molecular Life Sciences, Radboud University Nijmegen Medical Center
PO Box 9101, 6500 HB Nijmegen, the Netherlands

TRPM7 is an ubiquitously expressed non-specific cation channel that has been implicated in cellular Mg^{2+} homeostasis. We recently showed that moderate overexpression of TRMP7 in neuroblastoma N1E-115 cells elevates Ca^{2+} levels and markedly increases cell-matrix adhesion. We also found that activation of TRPM7 by phospholipase C (PLC)-coupled receptors further increased Ca^{2+} levels and augmented cell adhesion and spreading in a Ca^{2+}-dependent manner (Clark et al., 2006).

Regulation of the TRMP7 channel is not well understood, although it has been reported that PIP_2 hydrolysis closes the channel. We here addressed TRPM7 regulation by GPCR agonists. Using FRET assays for second messengers we show that TRPM7-dependent Ca^{2+} increases correlate with PLC activation, but not with other GPCR signaling cascades. In non-invasive "perforated-patch clamp" recordings TRPM7 currents are also activated by PLC agonists. Whereas we could confirm that, under whole-cell conditions, the channels were significantly inhibited by PLC-activating agonists, TRPM7 current inhibition by PIP_2 hydrolysis was only observed when $[Mg^{2+}]_i$ was reduced below physiological levels. Thus, under physiological $[Mg^{2+}]_i$ conditions, TRPM7 currents are activated rather than inhibited by PIP_2-hydrolyzing agonists.

Introduction

TRPM7 is an ubiquitously expressed non-specific cation channel that, intriguingly, contains a C-terminal serine-threonine kinase domain. It belongs to the TRPM (Melastatin-related) subfamily of Transient Receptor Potential (TRP) channels that transduce sensory signals (Clapham, 2003). TRPM7 appears essential for life in that knock-out or overexpression of the channels caused growth arrest, loss of adhesion and rapid cell death (Nadler et al., 2001; Schmitz et al., 2003; Su et al., 2006). We recently discovered that low-level overexpression of TRMP7 induces cell spreading and adhesion and that its´ activation by PIP_2-hydrolyzing receptor agonists leads to the formation of adhesion complexes in a kinase-dependent manner (Clark et al., 2006).

Currents of TRPM7 channels exogenously expressed in mammalian cells have been analysed by several groups. In physiological solutions, the channel conducts mainly Ca^{2+} and Mg^{2+} (Runnels et al., 2001), but in the absence of these divalents K^+ and Na^+ (Nadler et al., 2001; Runnels et al., 2001) are passed efficiently. A characteristic feature is the inhibition of this current by physiological intracellular Mg^{2+} levels: in whole-cell patch clamp experiments, large outward rectifying TRPM7 currents (Runnels et al., 2001; Nadler et al., 2001; Kerschbaum et al., 2003) are revealed by perfusion with Mg^{2+}-free pipette solutions. Furthermore, MgATP and MgGTP also inhibit the channels (Nadler et al., 2001; Demeuse et al., 2006) although some controversy was raised on this topic (Kozak et al., 2002). TRPM7 currents have been termed MagNuM (for Mg^{2+}-Nucleotide sensitive Metal ion (Nadler et al., 2001)) or MIC (for Mg^{2+}-Inhibited Cation (Kozak et al., 2002)) currents. These terms will here be used interchangeably to reflect whole-cell currents evoked by internal Mg^{2+} depletion. MagNuM/MIC currents revert around 0 mV; the inward currents are predominantly carried by divalent cations, whereas outward currents consist mainly of monovalent cations (at low $[Mg^{2+}]_i$). TRPM7 currents lack voltage- and time-dependent

activation (Nadler et al., 2001; Runnels et al., 2001), and outward rectification is most likely due to divalent permeation block of inward currents at negative potentials (Nadler et al., 2001). Accordingly, perfusion with divalent-free extracellular solutions augments inward currents and causes the I/V relationship to become linear. The activation of TRPM7 by internal perfusion with Mg^{2+}-free solutions does not rely on permeation block, but the precise mechanism of action has not been solved yet (Kozak et al., 2002). Several reports document that the setpoint for $[Mg^{2+}]_i$ sensitivity is governed by the kinase domain; however, constructs lacking the entire kinase domain can still be activated by internal Mg^{2+} depletion (Schmitz et al., 2003; Schmitz et al., 2005; Matsushita et al., 2005). Thus, the interactions of TRPM7 with Mg^{2+} are complex: Mg^{2+} is conducted through the channel pore, causes voltage-dependent permeation block, and influences gating at the cytosolic surface.

The exact mechanisms by which receptor agonists regulate TRPM7 are less well characterized and the published data are, at least partly, conflicting. An initially claimed indispensable role for the kinase domain (Runnels et al., 2001) was challenged in subsequent studies (Schmitz et al., 2003; Takezawa et al., 2004; Matsushita et al., 2005; Schmitz et al., 2005). Rather, we recently showed that the TRPM7 α-kinase specifically phosphorylates the heavy chain of myosin-II (Clark et al., 2006) thereby strongly influencing cell adhesion. Importantly, association with- and subsequent phosphorylation of myosin-II depend on prior activation of the channel by PLC-coupled receptors, and influx of extracellular Ca^{2+} constitutes an essential step in this process (Clark et al., 2006). In accordance, TRPM7 binds directly to several PLC isoforms, including PLCγ and PLCβ (Runnels et al., 2002). The stimulatory effect of PLC on TRPM7 observed in intact cells by biochemical-, cell-biological- and live-cell imaging studies contrasts markedly with a report by Runnels et al (Runnels et al., 2002) that in HEK-293 cells whole-cell TRPM7 currents are potently inhibited by carbachol-induced PIP_2 hydrolysis. PIP_2-dependent gating also occurs in other TRP family members, including TRPV1 (Prescott and Julius, 2003), TRPM5 (Liu and Liman, 2003) and TRPM8 (Liu and Qin, 2005; Rohacs et al., 2005). Finally, in a recent study Takezawa and colleagues (Takezawa et al., 2004) reported that in HEK-293 cells (expressing only endogenous muscarinic receptors) carbachol attenuated TRPM7 currents via the G_s-cAMP signalling pathway, whereas PLC activation was not involved.

As thus regulation of TRPM7 detected in whole-cell experiments appears to differ from our cell-biological studies, we here address the effects of GPCR stimulation by non-invasive techniques in cells retrovirally transduced to overexpress TRPM7 at very low level. We combine FRET assays for second messengers with Ca^{2+} fluorometry and perforated-patch experiments to show that opening of TRPM7 correlates well with PLC, but not with cAMP or cGMP signaling. We also address why in our observations the effect of PLC activation appears opposite to that obtained in whole-cell by comparing both approaches under various ionic conditions. Strikingly, in perforated patches TRPM7 currents can be evoked by treatment with the membrane-permeable Mg^{2+} chelator EDTA-AM, and these currents are inhibited, rather than augmented, by PLC-activating agonists. We conclude that in intact cells TRPM7 currents are enhanced, rather than inhibited, by PLC-coupled agonists.

Methods

Materials

Amphotericin B, MgATP, bradykinin, lysophosphatidic acid, spermin, $La(NO_3)_3$, $Gd_2(CO_3)_3$, sodium nitroprusside, prostaglandin E1, and niflumic acid were from Sigma-Aldrich Co. (St. Louis, MO). Oregon Green 488 BAPTA-1 AM, Fura Red AM, Indo-1 AM, o-nitrophenyl-EGTA AM, pluronic F127 and BAPTA-AM were from Molecular Probes Inc. (Eugene, OR). Ionomycin, 2-APB, SKF 96365, IBMX, forskolin, neurokinin A (NKA) and thapsigargin were from Calbiochem-Novabiochem Corp. (La Jolla, CA). Salts were from Merck (Darmstadt, Germany). Dulbecco's MEM, foetal calf serum, penicillin and streptomycin were obtained from Gibco BRL (Paisley, Scotland). Neomycin was purchased from Invitrogen-Life technologies (Breda, the Netherlands). FuGene 6 transfection reagent was from Roche Diagnostics B.V. (Penzbreg, Germany)

Constructs

Mouse TRPM7 in pTracer-CMV2 was a kind gift from Dr. D. Clapham (Harvard, Boston, Ma). To generate retroviral expression vectors, the TRPM7 cDNA was inserted as an *Xho*I-*Not*I

fragment into the LZRS-ires-neomycin vector. For production of recombinant protein in bacteria a pcr product encoding amino acids 1748 to 1862 of TRPM7 was cloned in frame in pGEX-1N using *Bam*HI and *Eco*RI sites. All constructs were verified by sequencing. The PIP_2 FRET sensor (eCFP-PHδ1 and eYFP-PHδ1) was previously generated in our lab as described (van der Wal et al., 2001). The genetically encoded cAMP sensor was a kind gift from Dr. M. Zaccolo (University of Padova, Padova, Italy), the cGMP sensor Cygnet 2.1 was kindly provided by Dr. W. Dostmann (University of Vermont, Burlington, VT), and the Ca^{2+} indicator Yellow Cameleon 2.1 was a gift from Dr. R. Tsien (UCSD, La Jolla, CA).

Cell Culture

Mouse N1E-115 and Phoenix packaging cells were cultured in DMEM supplemented with 10% fetal calf serum, penicillin and streptomycin and kept in a humidified CO_2 incubator. Stable cell lines were generated by retroviral transduction as previously described (Clark et al., 2006). Cells were selected by the addition of 0.8 mg/ml G418 to the media and the selection was complete within 7 days. Cells were passaged twice a week and seeded on glass cover slips for experiments.

Generation of Antibodies

To generate anti-TRPM7 antibodies, a GST-fusion protein encoding amino acids 1748 to 1862 was expressed in *Escherichia coli* BL21 and purified on a glutathione-sepharose column. Rabbits were injected with the antigen mixed with Freund's adjuvant and serum was collected 10 days after every vaccination. Serum collected before immunization (preimmune) was used as a control in all experiments (Clark et al., 2006).

In Vitro Kinase Assay

Cells were lysed in RIPA buffer (50 mM Tris pH 7.5, 150 mM NaCl, 0.1% SDS, 0.5% sodium deoxycholate, 1% triton X-100 supplemented with protease inhibitors), incubated on ice for 20 min, and lysates were cleared by centrifugation. Lysates were incubated with anti-TRPM7 antibodies for 3 h at 4°C and immunocomplexes were isolated by the addition of protG-sepharose. The beads were washed 3 times with lysis buffer and subsequently twice with kinase buffer without ATP (50 mM HEPES pH 7.0, 3.5 mM $MnCl_2$, 5 mM DTT). The kinase reaction was initiated by adding 0.1 mM ATP in combination with 5 μCi γ-^{32}P-ATP and proceeded for 30 min at 30°C. The products of the kinase reaction were resolved by SDS-PAGE on a 6% acrylamide gel and detected using a phosphoimager.

Immunolabeling of N1E-115/TRPM7 Cells

Cells grown for 24 hours on glass coverslips were fixed for 10 minutes at room temperature in phosphate-buffered saline and 4% paraformaldehyde. Subsequently, cells were permeabilized with 0.1% triton X-100 in phosphate-buffered saline. Cells were incubated with rabbit anti-TRPM7 sera (1:200) followed by horse-radish peroxidase-conjugated anti-rabbit Ig (1:1000). Amplification of the signal was by tyramide-conjugated FITC (PerkinElmer, Boston, MA) and images were collected using a Leica SP2 confocal microscope.

Ca^{2+} Determinations and Uncaging Experiments

For Ca^{2+} recordings, cells on glass coverslips were incubated for 30 min with dyes, followed by further incubation in medium for at least 15 min. For pseudoratiometrical determinations (van der Wal et al., 2001; Jalink et al., 1990), a mixture of 1 μg Oregon Green 488 BAPTA-AM and 4 μg Fura Red-AM in 100 μl medium was used. Coverslips were mounted on the inverted microscope and recordings were made at 37°C in HEPES-buffered saline, composed of (in mM): NaCl (140), KCl (5), $MgCl_2$ (1), $CaCl_2$ (1), HEPES (10) and glucose (10), pH 7.2. Single-cell fluorescence recordings were collected with a Nikon inverted microscope fitted with a Biorad MRC600 scanhead (Biorad, Herts, England). Excitation of Oregon Green and Fura-Red was at 488 nm and emission was detected at 522 +/- 16 nm and at >585 nm. All traces were calibrated with respect to maximal ratio (after ionomycin treatment) and minimal ratio (in the presence of excess BAPTA). Calculation of Ca^{2+} concentrations were performed as published (Grynkiewicz et al., 1985). Ca^{2+} experiments were also repeated in large series of ratiometric Indo-1 experiments, as well as using the FRET Ca^{2+} sensor Yellow Cameleon 2.1 (Miyawaki et al., 1997) essentially as published (van der Wal et al., 2001). For Ca^{2+} uncaging experiments, oNP-

EGTA (0.5 μg per 100 μl) was co-loaded with Ca^{2+} dyes into cells. Uncaging of oNP-EGTA was achieved by a sub-second flash of UV light (355 ± 25 nM) from a mercury arc lamp.

Indo-1 Quenching Experiments

N1E-115/TRPM7 cells on rectangular coverslips were grown to near-confluency. Cells were loaded with Indo-1 AM (1.5 μg/100μl) for 30 min and further incubated in fresh medium for at least 30 min. Coverslips were introduced into a photon-counting spectrofluorometer (Quanta-Master, PTI Inc., Lawrenceville, NJ) controlled by the vendors Felix software. Experiments were performed in HEPES-buffered saline; excitation was at 338 nm and emission was detected at 410 nm. Following recording of basal fluorescence changes for ~10 min, 200 μM Mn^{2+} was added and fluorescence was recorded for 10 more min. Autofluorescence, as determined by maximal quenching of Indo-1 with ionomycin + excess Mn^{2+}, was usually less than 10 %. Both the baseline and the initial part of the response after Mn^{2+} addition were fitted linearly, and the Mn^{2+}-induced quench rate was calculated by subtracting the former from the latter. The quench rate is expressed as decrease in detected photons (counts) per second.

Dynamic FRET Essays

Cells grown on coverslips were transfected with FRET constructs (1μg/coverslip) using FuGene 6 according to manufactures' guidelines, and experiments were performed as described previously (van der Wal et al., 2001; Ponsioen et al., 2004). In brief, coverslips were placed on an inverted Nikon microscope and excited at 425nm using an ND3 filter. CFP- and YFP emission were collected simultaneously through 470 ± 20 and 530 ± 25 nm bandpass filters. Data were acquired at 4 samples per second and FRET was expressed as ratio of CFP to YFP signals. This ratio was set to 1.0 at the onset of the experiments, and changes are expressed as per cent deviation from this initial value.

Patch-clamp Experiments

Electrophysiological recordings were collected using an EPC9 amplifier (HEKA electronics, Lambrecht, Germany), connected to a personal computer and controlled by HEKA pulse software. Voltage-clamp protocols were generated using HEKA pulse software, and current recordings were digitized at 100 kHz (ramp and block pulse protocols) or 10 Hz (steady-state whole-cell currents). Borosilicate glass pipettes were pulled on a p-2000 pipette puller (Sutter instruments, Novato, CA) and fire-polished (Narishige Microforge, Tokyo, Japan) to 2-4 MΩ. After establishment of the GΩ seal, the patched membrane was ruptured by gentle suction to obtain whole-cell configuration, or amphotericin B (240 μg/ml) was used to obtain the perforated-patch configuration with typical access resistance of 3-10 MΩ.

Solutions were as follows (in mM): whole-cell pipette solution: K-Glutamate (120), KCl (30), $MgCl_2$ (1), $CaCl_2$ (0.2), EGTA (1), HEPES pH.7.2 (10) and MgATP (1); external solution: NaCl (140), KCl (5), $MgCl_2$ (0-1), $CaCl_2$ (0-10), HEPES (10) and glucose (10), adjusted to pH 7.3 with NaOH; for perforated-patch recordings, the pipette solution was complemented with 240 μg/ml Amphotericin B and MgATP was omitted. For MIC/MagNuM recordings (Fig. 1*c & d*) the pipette solution contained CsCl (120), HEPES (10), MgATP (1) and $MgCl_2$ (0-3), pH adjusted to 7.2 with CsOH, and cells were kept in a solution containing TEACl (100), CsCl (5), $CaCl_2$ (2), $MgCl_2$ (1), HEPES (15), Glucose (10), pH adjusted with TEAOH to 7.3.

Results and Discussion

TRPM7 Expression Causes Increased MIC/MagNuM Currents

Consistent with observations by others (Nadler et al., 2001) we observed that transient overexpression of TRPM7 channels was lethal within 1 to 3 days in N1E-115 cells and all other cell lines tested (data not shown). Furthermore, at early time points after transfection, the protein located primarily to the biosynthetic pathway, with little or no expression detectable at the plasma membrane. To circumvent these problems, we introduced TRPM7 in N1E-115 cells at low expression levels by retroviral transduction. These cells, termed N1E-115/TRPM7 cells, were viable, divided normally and could be routinely kept in culture for several months. Using a TRPM7-specific antibody, the expression level in N1E-115/TRPM7 cells was found to be 2-3 times that of parental cells (Fig. 1*a*). As shown in Fig. 1*b*, the

majority of TRPM7 labeling localized to the plasma membrane.

Initially we analyzed whether TRPM7 overexpression caused in increased MIC/MagNum currents. In whole-cell patch clamp experiments, $[Mg^{2+}]_i$ was lowered by omission of the ion from the pipette solution. With a fluorescent dye in the pipette it was verified by confocal microscopy that intracellular perfusion was near-complete within a few minutes (data not shown). Concomitantly, both in parental and in N1E-115/TRPM7 cells, MIC/MagNuM currents developed. In parental cells, the current density at –60 mV averaged -0.33 +/- 0.08 pA/pF, N = 14 (Fig. 1*c*, *upper panel*; quantification in Fig. 1*d*). In N1E-115/TRPM7 cells, MIC/MagNuM current density averaged -0.80 +/- 0.18 pA/pF, N = 9 (Figs. 1*c*, *middle panel*, 1*d*), in good agreement with the expression data (Fig. 1*a*). In both cell lines, currents had all the characteristic hallmarks of MIC/MagNuM currents: first, they were strongly blocked by including 1-3 mM of free Mg^{2+} in the pipette solution (Fig. 1*c*, *lower panel*). Second, whole-cell currents showed an outward-rectifying I/V relationship in divalent-containing media (Fig. 1*e*) that became linear upon removal of divalents (Mg^{2+} and Ca^{2+}) from the medium (data not shown). Third, in line with the results from Runnels (Runnels et al., 2001), responses evoked by voltage-step protocols lacked voltage- or time-dependent characteristics (Fig 1*e*, *right panel*). Furthermore, sensitivity of MIC/MagNuM currents to inhibitors of TRPM7 matches with that reported in the literature (Table 1).

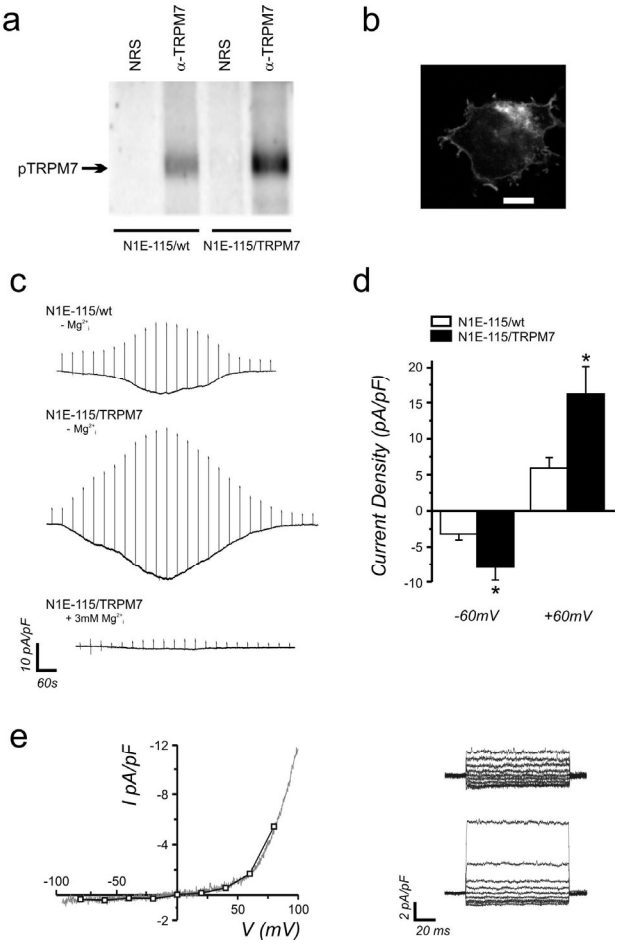

Fig. 1. Expression of TRPM7 in N1E-115 cells by retroviral transduction. *(a)* Retroviral transduction causes moderate overexpression of the TRPM7 channel-kinase as assayed by autophosphorylation of its kinase domain after immunoprecipitation by TRPM7-specific antibodies. *(b)* Confocal image of N1E-115 cell showing localization of the protein to the plasma membrane. TRPM7 was detected using anti-TRPM7 antibodies, followed by tyramide signal amplification. Scale bar, 10 μm. *(c) Upper panel*, MIC/MagNuM detected in whole-cell configuration. MIC/MagNuM currents start to develop immediately after break-in, peak at ~5-10 minutes and then gradually run down. Spikes represent current excursions induced by 1 s pulses to +60 mV from a holding potential of –60 mV. Solutions were chosen so that outward currents are mainly Cs^+, and inward currents are mainly Ca^{2+} by substituting tetraethyl ammonium (TEA^+) for Na^+ in the medium. *Middle panel*, MIC/MagNuM currents in N1E-115/TRPM7 cells are 2- to 3-fold larger in amplitude but display the same kinetics. *Lower panel*, inclusion of 3 mM Mg^{2+} in the pipette completely blocks MIC/MagNuM currents in N1E-115/TRPM7 cell. *(d)* Quantification of MIC/MagNuM currents for N1E-115/TRPM7 and parental cells, detected at –60 mV and at +60 mV. *: $p < 0.01$. *(e) Left panel*, I/V plots of MIC currents measured in N1E-115/TRPM7 cells by ramps (-100 to +100 mV, grey line) from at 0 mV holding potential and from instantaneous V-steps (20 mV-steps from –80 mV to 80 mV, black squares), corrected for background. Note complete overlap of I/V-plots obtained by these two methods. *Right panel*, individual, uncorrected traces from step-response currents at onset of the experiment (*top panel*) and at maximal activation (*lower panel*) show lack of time-dependent activation. Shown are representative traces from 10 individual experiments.

Table 1: Pharmacological characterization of TRPM7 currents as detected by different techniques

	Confocal Calcium	Whole cell	Perforated Patch
La^{3+} / Gd^{3+}	+ (200uM)	+ (5mM)	n.t.
2-APB (100μM)	+	+	+
SKF 96365 (30μM)	+	+	+
Spermin (50μM)	n.a.	+	n.t.
Niflumic acid (100μM)	+	+	+

N1E-115/TRPM7 cells were challenged with 1 μM bradykinin and the sensitivity of the ensuing sustained responses to the indicated blockers was tested. +, response is sensitive to blocker; n.a., not applicable (i.e. spermin works only in divalent-free media); n.t., not tested. All experiments were performed at least in triplicate.

Elevated Basal and Agonist-Induced Cytosolic Ca^{2+} Levels in N1E-115/TRPM7 Cells

Next we analyzed $[Ca^{2+}]_i$ in parental and N1E-115/TRPM7 cells by ratiometrical Ca^{2+} imaging (see Methods). Intracellular Ca^{2+} was elevated significantly in N1E-115/TRPM7 cells (108.9 +/- 6.0 nM, N = 50) as compared to parental cells (85.3 +/- 2.5 nM, N = 50; $p < 0.05$; Fig. 2*a,* quantification in *Fig. 2b*). As it has been reported that TRPM7 channels are partly pre-activated (Schmitz et al., 2003; Kozak and Cahalan, 2003; Hanano et al., 2004; Matsushita et al., 2005; Demeuse et al., 2006), this suggests that in N1E-115/TRPM7 cells too, a part of the TRPM7 channel population is open under resting conditions. Thus, low-level overexpression of TRPM7 is well tolerated and contributes to Ca^{2+} homeostasis.

Because cell-biological and biochemical data (Clark et al., 2006) indicate that TRPM7 channels are activated by the GPCR agonist BK, we next monitored the effect of addition of BK on TRPM7-mediated Ca^{2+} influx by comparing N1E-115/TRPM7 to parental cells. In N1E-115 cells, stimulation of endogenous B2 receptors with bradykinin (BK) strongly activates PLC through the G_q pathway (Coggan and Thompson, 1995; Chapter II). In parental cells, 1 μM BK induced a cytosolic Ca^{2+} increase (765.9 +/- 9.7 nM, N = 80) that peaked within seconds and subsequently returned to values close to resting levels (92.9 +/- 2.9 nM) within 60s (Fig. 2*a*, *left panel*). This corresponds to a mean increase of 7.6 nM from basal levels, which was not statistically significant. In contrast, in N1E-115/TRPM7 cells the BK-induced transient Ca^{2+} increase (peak 843.3 +/- 12.7 nM) was followed by a prominent sustained Ca^{2+} elevation (141.0 +/- 7.0 nM, N = 120) that lasted for several minutes before returning to resting levels rather abruptly (Fig. 2*a*, *right panel*; quantification in Fig. 2*b*). Note that, in comparison with wt cells, the magnitude of the mean increase in sustained Ca^{2+} levels in N1E-115/TRPM7 cells (32.1 nM; $p < 0.001$, paired t-test) corresponds reasonably well with the 2 to 3-fold higher TRPM7 expression levels. Thus, expression of TRPM7 at the plasma membrane elicits a sustained phase in the Ca^{2+} response to BK, in good agreement with

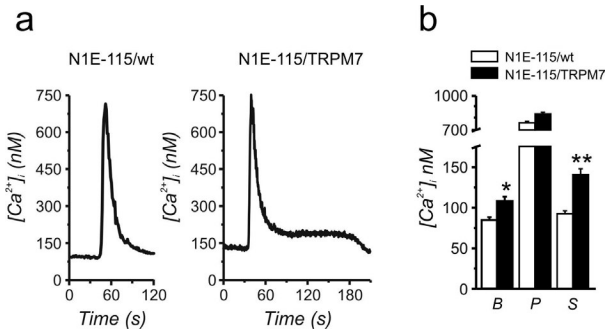

Fig. 2. Sustained Ca^{2+} influx in N1E-115/TRPM7 cells after stimulation of PLC. *(a)* Pseudo-ratiometric single-cell Ca^{2+} traces showing effect of addition of bradykinin (BK, 1 μM) in parental (*left panel*) and TRPM7 transduced cells (*right panel*). Note the characteristic abrupt end of the sustained phase after ~3-5 minutes. Shown are representative traces from hundreds of experiments. Similar results were obtained with Indo-1 as well as with the FRET Ca^{2+} sensor Yellow Cameleon 2.1 (see Methods). *(b)* Effects of retroviral TRPM7 expression on basal (B) and agonist-induced peak (P) and sustained (S, taken 2 minutes after addition of BK) calcium levels. $[Ca^{2+}]_i$ concentrations were calibrated with ionomycin and BAPTA, and data of hundreds of cells were averaged. Shown are mean + s.e.mean of values of the initial Ca^{2+} peak and of the sustained phase, taken 2 minutes after addition of BK. *: $p < 0.001$.

our cell-biological data (Clark et al., 2006).

BK-Induced Sustained Ca^{2+} Elevation Is Due to Influx Through TRPM7

To address whether the sustained Ca^{2+} phase is due to entry through TRPM7 channels, we investigated several alternatives. First, it is conceivable that expression of TRPM7 could burden the cells with excess Ca^{2+} entry, thereby compromising intracellular Ca^{2+} buffering mechanisms. Therefore we assayed cytosolic Ca^{2+} buffering by quantitating the rate of clearance of UV-released caged Ca^{2+}. Native N1E-115 and N1E-115/TRPM7 cell were loaded with o-nitrophenyl-EGTA and Ca^{2+} dyes (see Methods) and exposed to ~0.2s flashes of UV light (Fig. 3*a, left and middle panels*). In wt cells, this caused an instantaneous increase in $[Ca^{2+}]_i$, which was cleared from the cytosol with a time course well fitted by a single exponential. Ca^{2+} drop rates in both cell lines were indistinguishable (21.77 +/- 2.00, N = 15 versus 21.75 +/- 1.76, N = 15, Fig. 3*a*, *right panel*), ruling out different cytosolic buffering as the responsible mechanism. Note that the shape of the BK-induced Ca^{2+} increase, with a prolonged sustained phase that ends rather abruptly after several minutes (Fig. 2*a, right panel*), also argues against flawed Ca^{2+} buffering as the responsible mechanism. Rather, sustained elevated $Ca^{2+}{}_i$ levels are due to influx since they were absent in cells acutely pre-treated with the calcium chelator BAPTA at 3 mM (Fig. 3*b, left panel*). Addition of BAPTA during the sustained Ca^{2+} elevation also caused a rapid drop which often proceeded to values below basal level (Fig. 3*b, right panel*; 59.9 +/- 8.2 nM), an observation that is in line with the reported pre-activation of TRPM7 channels. Thus, the sustained phase in BK-stimulated N1E-115 cells reflects Ca^{2+} influx over the plasma membrane.

We further ruled out that addition of BK caused depolarization of the cell membrane with consequent Ca^{2+} influx through voltage-sensitive Ca^{2+} channels. Whereas this has been described for N1E-115 cells that were induced to adopt a differentiated neuronal phenotype (Bolsover, 1986) by 2-4 day serum starvation, in non-starved cells $Ca^{2+}{}_i$ levels were completely insensitive to depolarization by 50-100 mM extracellular K^+ (Fig. 3*c*). Furthermore, resting membrane potentials of non-starved native and TRPM7 overexpressing cells did not differ (-29.9 +/- 3.4 mV and -32.8 +/- 5.3 mV, resp.) and BK stimulation evoked only minor depolarization of the plasma membrane (wt: 10.0 +/- 4.0 mV, N=6; N1E-115/TRPM7: 11.8 +/- 0.9 mV, N=5). These results rule out activation of a voltage-sensitive Ca^{2+} channel as the responsible mechanism and are in line with the reported lack of voltage sensitivity of TRPM7 at physiological membrane voltage.

Finally, we tested sensitivity of the sustained phase of Ca^{2+} influx to a panel of inhibitors for TRPM7 channels (Table 1). When administered during the sustained Ca^{2+} phase, 2-aminoethoxy-

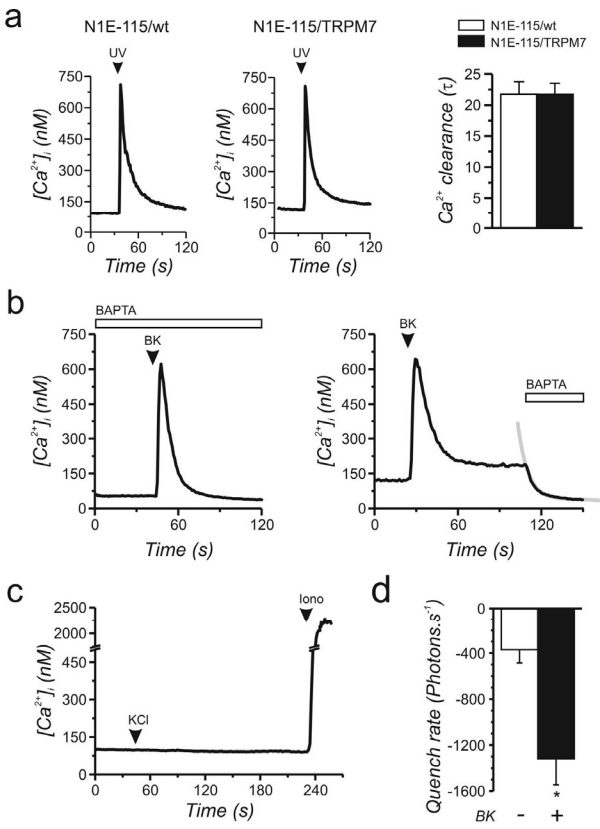

Fig. 3. Sustained Ca^{2+} levels in N1E-115/TRPM7 cells are due to increased membrane permeability. (*a*) *Left and middle panel*, typical traces showing similar Ca^{2+} clearance of caged Ca^{2+} spikes in parental and N1E-115/TRPM7 cells. *Right panel,* quantification (mean + s.e.mean of τ; N = 15) of Ca^{2+} clearance from single-exponential fits. (*b*) *Left panel*, sustained Ca^{2+} elevation after BK stimulation in N1E-115/TRPM7 cells is abolished by brief pre-treatment with extracellular BAPTA. *Right panel*, addition of BAPTA during the sustained Ca^{2+} phase lowers $[Ca^{2+}]_i$ to values below baseline. (*c*) Depolarization of N1E-115/TRPM7 cells by adding extracellular KCl (50mM) does not cause Ca^{2+} influx; iono indicates addition of the Ca^{2+} ionophore ionomycin as a positive control. Note the break in the Y-axis. (*d*) BK (1 μM) stimulation causes increased permeability for Mn^{2+} in N1E-115/TRPM7 cells as measured by an Indo-1 quenching assay (mean + s.e.mean; N = 6; *: $p < 0.025$, single-sided t-test).

diphenyl-borate (2-APB, 50μM) (Jiang et al., 2003) completely blocked BK-induced Ca^{2+} influx. In line with the observation that TRPM7 expression also contributes to basal Ca^{2+}_i levels, the 2-APB-induced drop in Ca^{2+} levels often proceeded to values below baseline (data not shown). Furthermore, we tested SKF 96365 (30μM) (Kozak et al., 2002), and the polyvalent cations Gd^{3+} and La^{3+} (both at 200μM) (Runnels et al., 2001). In all cases, the BK-induced sustained phase, but not the initial Ca^{2+} peak, was strongly inhibited. Note that none of these inhibitors are truly selective for TRPM7, and that this pharmacological profile also fits I_{CRAC}. However, unlike I_{CRAC} (Hoth and Penner, 1992) TRPM7 permeates Mn^{2+} ions well (Monteilh-Zoller et al., 2003). When tested by Indo-1 quenching assays (see Methods), N1E-115/TRPM7 cells challenged with BK were significantly more permeable to Mn^{2+} than unstimulated cells (Fig. 3*d*). Taken together, these data strongly suggest that the BK-induced sustained Ca^{2+} elevation in N1E-115/TRPM7 cells is mediated by influx through TRPM7 channels in the plasma membrane.

TRPM7 Activation in Intact N1E-115 Cells Is Downstream of G_q/PLC Signaling

In whole-cell patch clamp experiments on HEK-293 cells overexpressing M1 muscarinic receptors, TRPM7 channels were shown to be inhibited by carbachol-induced PIP_2 breakdown (Runnels et al., 2002), and this inhibition was reverted by intracellular perfusion with a water-soluble PIP_2 analogue. This result was subsequently challenged by Takezawa and colleagues (Takezawa et al., 2004) who found that activating PLC through endogenously expressed M1 receptors had little effect on TRPM7 currents, and used the lack of effect of the inhibitor U-73122 to underscore this point of view. Instead, they reported that whole-cell TRPM7 currents were enhanced or attenuated, respectively, by agonists to receptors that couple to stimulatory (G_s) or inhibitory (G_i) G proteins to raise or lower intracellular cAMP levels.

We made use of the endogenously expressed B2 bradykinin receptors that couple predominantly to the G_q/PLC pathway, but some scattered reports suggest that depending on the cell type the B2 receptor may sometimes either inhibit (Hanke et al., 2001) or stimulate (Albert et al., 1999) production of cAMP. Hence, we set out to identify

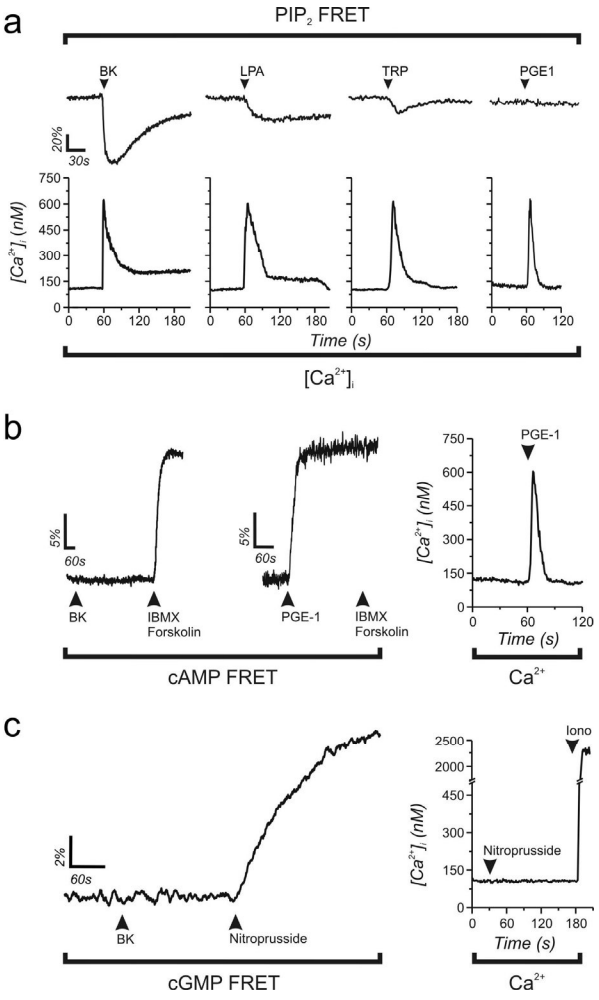

Fig. 4. Activation of TRPM7 by GPCRs: involvement of the G_q / PLC signalling pathway. (*a*) Representative FRET traces showing PIP_2 hydrolysis (*upper panel*) induced by BK, LPA and thrombin receptor activating peptide (TRP), and the ensuing sustained Ca^{2+} elevations in N1E-115/TRPM7 cells (*lower panel*). Prostaglandin E1 (PGE-1), a potent activator of cAMP production, does not activate PLC and it fails to evoke sustained Ca^{2+} entry (*rightmost traces*). (*b)* BK receptor activation does not alter cAMP levels in N1E-115/TRPM7 cells as detected by a PKA-based FRET probe *(left panel)*. Addition of the adenylyl cyclase activator forskolin together with the phosphodiesterase inhibitor IBMX serve as a positive control. Conversely, PGE-1 potently activates the G_s / cAMP pathway through its cognate GPCR *(middle panel)* but fails to elicit the sustained Ca^{2+} elevation *(right panel)* that is typically seen after G_q / PLC activation. (*c*) In N1E-115/TRPM7 cells BK fails to alter cGMP levels, whereas the NO-donor nitroprusside readily activates this pathway, as assessed using Cygnet, a FRET sensor for cGMP (Honda et al., 2001). Addition of nitroprusside had no effect on $[Ca^{2+}]_i$ in these cells *(right panel)*.

the signaling route responsible for BK-induced activation of TRPM7 in intact N1E-115/TRPM7 cells by correlating Ca^{2+} fluorometry with activation of intracellular signaling pathways, as detected by various FRET assays.

We and others have previously reported that stimulation of endogenous B2 receptors with BK causes rapid breakdown of a significant fraction (60-80%) of the membrane PIP_2 pool in N1E-115 cells (van der Wal et al., 2001; Xu et al., 2003). Similarly, addition of BK to N1E-115/TRPM7 cells caused near-complete breakdown of PIP_2, as detected by a FRET assay that reports membrane PIP_2 content (Fig. 4*a*, *upper panel, first trace* (van der Wal et al., 2001)). In these cells, the G_q-coupled agonists lysophosphatidic acid (LPA) and thrombin receptor activating peptide also activate PLC, albeit to a lesser extent (~20-30% of BK values; N > 200; Fig. 4*a*, *upper panel, second and third trace* (van der Wal et al., 2001)). Similar to BK, the initial Ca^{2+} peak induced by these agonists was followed by sustained Ca^{2+} influx in N1E-115/TRPM7 cells, although responses were a bit more variable than those to BK (Fig. 4*a, lower panel*). In contrast, sustained Ca^{2+} influx was not seen when cells were stimulated with agonists to receptors that do not couple to PLC (Fig. 4*a*, *right panel*, and data not shown). Thus, TRPM7 activation correlates well with PLC activation / Ca^{2+} signaling but it does not require near-complete breakdown of the PIP_2 pool.

To address possible involvement of cAMP in the BK-induced opening of TRPM7, we monitored cAMP levels in intact N1E-115/TRPM7 cells using a genetically encoded sensor for cAMP (Zaccolo et al., 2000). Of the available FRET sensors for cAMP, this sensor has the highest affinity (Kd of 300 nM (Bacskai et al., 1993)) and it is well suited to reveal small changes from baseline levels. Addition of BK to N1E-115/TRPM7 cells had absolutely no effect on cAMP levels (N = 8), whereas forskolin (25µM) readily raised cAMP levels in these cells (Fig. 4*b*, *left panel*). Furthermore, we tested the effects of pre-treatment of cells with pertussis toxin, which specifically inhibits G_i and thereby blocks receptor-induced decreases in cAMP levels, on the response to BK. No effects on kinetics or amplitude of the BK-induced Ca^{2+} influx were observed in N1E-115/TRPM7 cells (data not shown). Thus, we find no evidence that cAMP may mediate BK-induced opening of TRPM7. Conversely, we tested the effect of agonists that do signal potently through G_s and G_i, respectively. Prostaglandin E1 (PGE1) potently activates G_s to

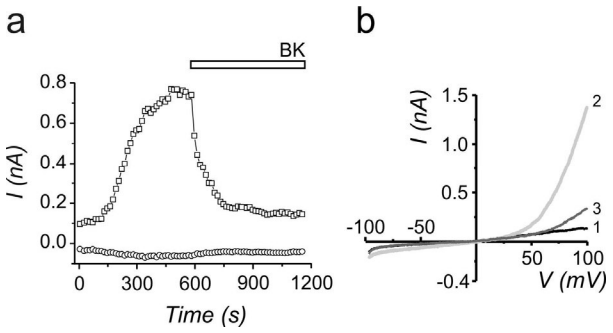

Fig. 5. MIC/MagNuM currents in N1E-115/TRPM7 cells are inhibited by BK. *(a)* TRPM7 currents, evoked with Mg^{2+}-free pipette solution in a N1E-115/TRPM7 cell, are strongly inhibited after activation of PLC. Currents evoked by ±100 mV ramps (*b*) from a holding potential of 0 mV are quantified at –80 mV (*circles*) and +80 mV (*squares*). Note that the small inward currents are due to divalent-block in Mg^{2+}- and Ca^{2+}-containing extracellular medium. Shown is a representative trace from 10 individual experiments.

cause a rapid and sustained increase in $[cAMP]_i$ (Fig. 4*b*, *middle panel*) that was not paralleled by sustained Ca^{2+} influx (Fig. 4*b, right panel*). Similarly, activation of G_i by Sphingosine-1-phosphate (S1P) was ineffective. We conclude that there is no evidence for a role of cAMP in BK-mediated Ca^{2+} influx in N1E-115/TRPM7 cells.

We also investigated the role of other well-delineated signaling pathways in N1E-115 cells. In these cells, stimulation with agonists that couple to G_{13} leads to strong activation of the small GTPase Rho, resulting in rapid contraction of the actin cytoskeleton (Postma et al., 1996b). S1P potently activates this signaling cascade (Postma et al., 1996b) but it does not couple to G_q (KJ, unpublished results). In N1E-115/TRPM7 cells, S1P caused rapid cytoskeletal contraction but it had no detectable effect on Ca^{2+} (data not shown). Finally we tested the effects of addition of the NO-donor nitroprusside since NO was reported to activate TRPM7-mediated Ca^{2+} influx in cultured cortical neurons (Aarts et al., 2003). In intact parental and N1E-115/TRPM7 cells, nitroprusside potently triggered production of cGMP (Methods; Fig. 4*c*, *left panel* (Ponsioen et al., 2004)) but no effect on $[Ca^{2+}]_i$ was observed (Fig. 4*c, right panel*). In conclusion, TRPM7 opening correlates well with G_q / PLC but not with other G-protein mediated signals in our cells.

Activation of PLC Inhibits Whole-cell TRPM7 Currents in N1E-115/TRPM7 Cells.

In whole-cell patch clamp experiments on HEK-293 cells overexpressing M1 muscarinic receptors, TRPM7 channels were shown to be inhibited by carbachol-induced PIP_2 breakdown (Runnels et al., 2002), and this inhibition was reverted by intracellular perfusion with a water-soluble PIP_2 analogue. This result contrasts with our cell-biological, biochemical and Ca^{2+}-data (see above, and (Clark et al., 2006)) that show that PLC activation causes opening rather than closure of TRPM7 channels. We therefore tested whether TRPM7 currents recorded in whole cells with Mg^{2+}-free pipette solution were similarly suppressed in our cells. Upon break-in, channel activation was monitored from outward-rectifying (MIC/MagNuM) currents evoked with voltage ramps. Indeed, challenging the cells with BK after full activation of TRPM7 caused currents to rapidly decrease in both native N1E-115 cells (data not shown) and N1E-115/TRPM7 cells (99.7 % ± 1.0, N=9, Fig. 5*a*). Whereas inward currents were completely abolished, small outward currents were still observed at high depolarizing potentials (Fig. 5*b, trace 3*). Other PLC-coupled agonists, including TRP and LPA, also inhibited the currents, though to a lesser extent. Therefore, it appears that the original observations on PIP_2-dependency of whole-cell TRPM7 currents hold true for N1E-115/TRPM7 cells.

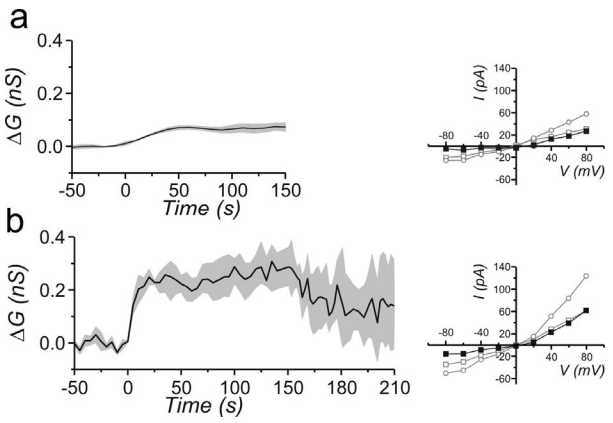

Fig. 6. TRPM7 currents detected using perforated-patch clamping. N1E-115 wt *(a)* and N1E-115/TRPM7 cells *(a)* were kept at a holding potential of –70 mV and membrane conductance changes were determined from current responses to biphasic +10 and –10 mV block pulses. Note the BK-induced sustained activation of an additional conductance (BK, 1 μM). To verify that the small BK-evoked current would suffice to increase $[Ca^{2+}]_i$ significantly, we point out that an influx of just 10 pA of current carried by Ca^{2+} equals 10 x 10^{-12} / F.z = 5 x 10^{-17} mole (F, faraday constant; z, valence of ion), which in a cell of 1 pl volume would raise $[Ca^{2+}]$ by 5 x 10^{-5} M (50 μM) in 1 second, if no buffer systems are in place. Weakly rectifying currents induced by BK in wt (Fig. 6*a*, *left panel*) and N1E-115/TRPM7 (Fig. 6*b*, *left panel*) cells obtained by subtracting unstimulated from stimulated I/Vs.

Gq-PLC Coupled Receptor Agonists Activate TRPM7 Currents in Intact Cells

The above observations leave us with a paradox: PLC activation inhibits TRPM7 currents in whole-cell experiments, whereas it opens the channels when assayed by Ca^{2+} fluorometry. What causes this difference? Immediately after breaking the patch membrane to whole-cell, perfusion will start to dilute diffusible signaling molecules, which could influence gating properties. To test this possibility, we analyzed the electrophysiological effects of PLC activation in intact cells using the perforated patch configuration (Rae et al., 1991; Postma et al., 1996a). In this configuration, conventional GΩ seals are obtained, but electrical access to the cell is gained by including selective Na^+/K^+ ionophores in the pipette solution, which incorporate in the patch membrane. Using amphotericin B, we routinely obtained access resistances well below 10 MΩ, allowing reliable recording of total membrane currents without disturbing the cytosolic composition.

Voltage clamped perforated patches were held at –70 mV, and conductance of the membrane was monitored by measuring currents evoked by a biphasic block-pulse protocol (+ 10 and –10 mV from resting potential; Fig. 6*a*). In unstimulated cells, evoked currents were small (0.46 +/- 0.16 pA/pF, N=10), corresponding to a membrane conductance of 23 pS/pF. Note that since Mg^{2+} levels are intact in the perforated-patch configuration, the magnitude of the detected currents should match those of whole-cell experiments with Mg^{2+} included in the pipette (Fig. 1*c*, *lower panel*). Indeed, the currents induced by 120 mV voltage steps in unstimulated whole-cells measured 3.1 +/- 0.4 pA/pF (N=5), which corresponds to ~26 pS/pF, in close agreement with the perforated-patch data. As to be expected, spontaneously developing currents were never observed in perforated patches (Data not shown). Strikingly, stimulation with bradykinin significantly increased the membrane conductance

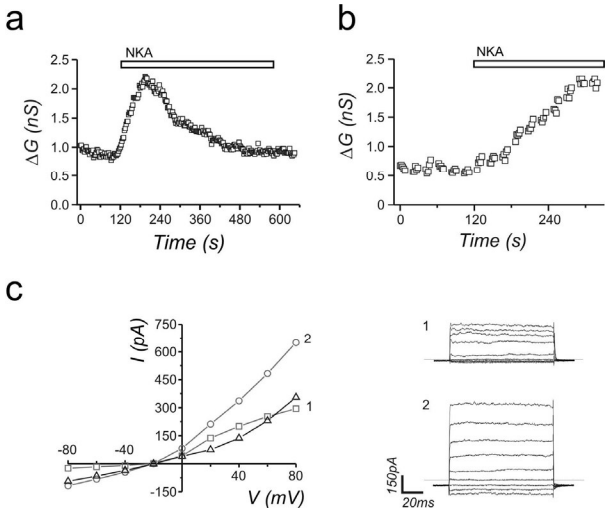

Fig. 7. TRPM7 current activation by NKA in HEK293 overexpressing TRPM7. (*a)* HEK-293 cells transiently expressing TRPM7 as well as NK2 receptors show increased membrane conductance upon stimulation of PLC with NKA (4 μM) in perforated-patch experiments. *(b)* In whole-cells with 1 mM of Mg^{2+} in the pipette solution, addition of NKA stimulates, rather than inhibits, TRPM7 currents. *(c) left panel*, I/V-plots from NK2-induced TRPM7 activation in HEK293 cells during whole-cell configuration. I/V-plots obtained before (1) and after (2) NKA stimulation. Black line, NKA-induced increase in currents (i.e., 1 – 2). Individual current responses to voltage steps *(right panel)* show all the hallmarks of TRPM7 currents.

(~250 +/- 53pS, N=6, Fig. 6*b*, *left panel*) in N1E-115/TRPM7 cells. In all cases, currents were transient, reverting to baseline with somewhat variable kinetics (range, 2-8 minutes). Note that whereas these conductance changes are quite small, the magnitude of inward currents, which are carried predominantly by Ca^{2+} (Nadler et al., 2001), is adequate to explain the sustained Ca^{2+} phase observed in fluorometric experiments (for analysis, see legend to Fig. 6). As wildtype N1E-115 cells express some endogenous TRPM7 channels, we next examined whether these are similarly activated after activation of PLC. Indeed, addition of BK increased the membrane conductance slightly, but significantly (Fig 6*a, left panel*). In addition, the same panel of inhibitors blocked the BK-induced currents (see Table 1). I/V plots of BK-induced currents in wt and N1E-115/TRPM7 cells revealed almost linear currents (Fig. 6*a and b*, *right panels*), the magnitude of which correlated with the expression levels. We conclude that bradykinin can activate TRPM7 channels in both native and TRPM7-transduced N1E-115 cells.

We next verified these results in HEK-293 cells. Cells were transiently transfected with TRPM7 (in a GFP-tagged zeocin vector) and the NK2-receptor, a G protein-coupled receptor (GPCR) for neurokinin A (Mau et al., 1990) that signals predominantly through G_q. One day after transfection, healthy cells expressing GFP at low levels were selected. When assayed by whole-cell patch clamping with Mg^{2+}-free pipette solutions, these cells displayed outwardly rectifying currents with all the hallmarks of TRPM7, including spontaneous activation and subsequent run-down (data not shown). In perforated-patch experiments, HEK-293 cells showed small, near-linear currents and no spontaneous developing outward rectifying currents were observed. Challenging HEK-293 cells with neurokinin A (NKA) caused a marked increase in membrane conductance (ΔG 0.79 +/- 0.33 nS; N = 3; Fig.7*a*). Again, conductance increases were transient, reverting to baseline within minutes. Note however, that in HEK-293 cells responses were quite variable, perhaps reflecting more widely diverging TRPM7 expression levels or impaired viability of transiently transfected cells. The inhibitor 2-APB (100 μM) consistently lowered the conductance to below initial values, in line with the notion that part of the channel population is opened under resting conditions (data not shown). Thus, the perforated-patch data obtained from HEK-293 cells transiently expressing TRPM7 match those obtained from N1E-115/TRPM7 cells, demonstrating that the phenotype does not depend on long-term viral transduction. We conclude that the stimulatory effect of PLC on TRPM7 currents in minimally perturbed cells parallels the Ca^{2+} imaging data, but contrasts with the data from $Mg^{2+}{}_i$-free whole-cell patch clamping.

The above observations suggest that in whole-cells, loss of $[Mg^{2+}]_i$ or possibly other signaling cofactors is sufficient to cause TRPM7 to become inhibited, rather than activated, by PLC activating agonists. To study this, HEK-293 cells transiently expressing TRPM7 were whole-cell patch-clamped with 1 mM free Mg^{2+} in the pipette. Under these conditions, NKA stimulation (Fig. 7*b*) also caused activation of TRPM7, as observed by the increase in membrane conductance. The I/V-plots obtained are slightly outward-rectifying, suggesting that internal Mg^{2+} partly prevents outward rectification by blocking/obstructing the pore of TRPM7 (Fig. 7*c*, *left panel*). Again, no voltage- or time-dependent components were observed in the current responses to voltage steps (Fig. 7*c*, *right panel*). Thus, stimulatory effects of PLC-activating agonists on TRPM7 currents can also be observed in whole-cells.

Concluding Remarks

In this study we addressed the regulation of TRPM7 channels in intact cells using low-level (2- to 3-fold) overexpression. Transient over-expression of the protein was avoided because this caused mislocalisation of TRPM7 to endo-membranes and cell death within a few days most likely because TRPM7 is to some extent constitutively active. Furthermore, transient overexpression is also more likely to titrate out essential binding partners and thereby influence signaling events. Indeed, Takezawa *et al.* noted that TRPM7 expression abolished activation of PLC by carbachol receptors (Takezawa et al., 2004). Strikingly, in a very recent study by Kim and colleagues (Kim et al., 2005) also concluded that regulation of native TRPM7 channels by PLC appeared different from results published previously from transiently transfected HEK293 cells (Runnels 2002). We furthermore chose to use perforated-patch clamping and Ca^{2+} imaging to avoid disturbing cell signaling due to intracellular perfusion in whole-cell configuration.

Our results revealed that retroviral transduction resulted in the appearance of a conductance with all the properties of TRPM7. The evidence can be summarized as follows. (i) The TRPM7 protein is expressed (Fig. 1*a*) and it resides at the plasma membrane (Fig. 1*b*). (ii) Its expression increases membrane permeability to Ca^{2+}, evident from increased basal Ca^{2+} levels (Fig. 2*a & b,*). (iii) Whole-cell currents in these cells have all the hallmarks of TRPM7 (Fig. 1*d & e*), i.e. activation by omitting Mg^{2+}_i from the pipette solution with subsequent run-down, reversal potential about 0 mV, and outward rectification that becomes linear when extracellular divalents are removed. Moreover, these currents are inhibited upon PLC activation as originally reported. (iv) The sensitivity of sustained Ca^{2+} influx and whole-cell currents to a panel of inhibitors (Table 1) corresponds to that reported earlier for TRPM7. Whereas I_{CRAC} is blocked by the same panel of inhibitors, it differs from TRPM7 in that it is hardly permeable to Mn^{2+} ions (Fig. 3*d*), and shows fast desensitization in divalent-free solutions. (v) The basal currents observed in perforated-patches (which are small due to intracellular Mg^{2+}, data not shown) have the same magnitude as the whole-cell currents in the presence of intracellular Mg^{2+} (Fig. 1*c*, *lower panel*), and BK-evoked additional currents, which are transient and revert to baseline levels within several minutes, have the same properties. (vi) In addition, we can rule out obvious other candidates such as compromised cytosolic Ca^{2+} buffering (Fig. 3*a*) and TRPM2 (which is also widely expressed, and was detected in N1E-115 by RT-PCR) that display linear I/V-relationship and are more Ca^{2+} selective (Perraud et al., 2001).

Of course the phenotype of TRPM7 in Ca^{2+} experiments strongly reminisces of Store-Operated Calcium Entry (SOCE, I_{CRAC}). SOCE is likewise manifested as a sustained plateau phase that depends on Ca^{2+} influx to follow an initial large Ca^{2+} peak from IP_3-sensitive internal stores. Unlike SOCE, however, TRPM7 opening was not evoked by depletion of stores with thapsigargin (Prakriya and Lewis, 2002; Hermosura et al., 2002) and data not shown). Moreover, under divalent-free conditions I_{CRAC} inactivates within seconds, whereas MIC/MagNum currents showed no decay for at least a few minutes. Furthermore, the relative permeability of TRPM7 channels to different ions does not fit with I_{CRAC}: TRPM7 channels are permeable to Mg^{2+}, Mn^{2+} (Fig. 3*d*) and Cs^{+} (Fig. 1*b & c*) whereas I_{CRAC} is characterized as non-permeable for these ions (Hoth and Penner, 1992; Zweifach and Lewis, 1993; Lepple-Wienhues and Cahalan, 1996). We thus arrive at the same conclusion as previous studies that point out that TRPM7 is not the channel responsible for conducting I_{CRAC} (Kozak et al., 2002; Prakriya and Lewis, 2002; Hermosura et al., 2002).

Two very recent reports strongly support the view that PLC activity augments, rather than inhibits, TRPM7 channels. Kim and colleagues showed that in clusters of interstitial cells of Cajal, which control pacemaking activity in the intestine, pacemaker frequency is determined by endogenous TRPM7 channels. Strikingly, addition of stem cell factor, a stimulus that causes PIP2 breakdown, positively influenced pacemaking, indicative of increased TRPM7 conductance in these cells (Kim et al., 2005). In a second report, we analyzed the role of TRPM7 in regulating actomyosin contractility (Clark et al., 2006). This report showed that upon stimulation of cells with PLC activating agonists such as bradykinin, the TRPM7 kinase domain associates with the actomyosin cytoskeleton in a Ca^{2+} and kinase-dependent manner. Within this complex, TRPM7 inhibits myosin-II function resulting in the transformation of focal adhesions into podosomes. These biochemical and cell biological data unequivocally demonstrate activation of native TRPM7 protein by PLC-activating agonists under physiological conditions.

Strikingly, and at odds with previous reports, we observed that stimulation of PLC-activating receptors caused TRPM7 channel opening rather than closure. This discrepancy is not cell type dependent because similar observations were made in N1E-115 and HEK-293 cells, nor does it depend on TRPM7 expression levels. Rather, it was found that in intact, minimally perturbed cells (Ca^{2+} imaging and perforated-patch) PLC-coupled agonists activated the channel, whereas upon prior channel opening by Mg^{2+}_i depletion (whole-cell) PLC activation potently inhibited MIC/MagNuM currents. Conceivably, Mg^{2+}_i levels act on the TRPM7 protein itself, because it was reported that mutations in the kinase domain altered the channels setpoint for Mg^{2+} inhibition (Schmitz et al., 2003). Alternatively, Mg^{2+} depletion might act by altering interaction with adenosine nucleotides (ATP, cAMP) or by influencing (Nadler et al., 2001; Demeuse et al., 2006) phosphoinositide metabolism, especially since both PIPkinases and PIP_2 phosphatases are strongly Mg^{2+} dependent (Ling et al., 1989). Analysis of the kinetics of BK-mediated stimulatory and inhibitory effects on TRPM7 shows that activation proceeds faster than inactivation. We speculate that this reflects fundamentally different modes of regulation mediating stimulation and inhibition, as opposed to a model whereby Mg^{2+}_i would modulate (flip) the effects of PLC activation on the channel. Rescue of agonist-induced channel inactivation by replenishment of membrane PIP_2 in Mg^{2+}-free inside-out patches (Runnels et al., 2002) shows that PIP_2 is an essential cofactor for channel opening. The precise mechanism of the activation pathway remains elusive, although we can exclude the involvement of the PIP_2-derived messengers DAG (since addition of membrane-permeable analogues did not activate TRPM7, data not shown) and cytosolic Ca^{2+} (Fig. 3*a*). In any case, we find that in unperturbed cells TRPM7 increases Ca^{2+}_i levels upon PLC activation and therefore we propose that this must be the more physiological mode of action.

Takezawa and colleagues recently reported that activation of PLC through endogenous M1-muscarinic receptors had little effect on MIC/MagNuM currents in TRPM7-overexpressing HEK-293 cells (Takezawa et al., 2004). Perhaps the discrepancy between Runnels' and our study on the one hand, and that of Takezawa and colleagues on the other hand, is a difference in potency of the PLC-activating receptors involved as in their (and our) hands endogenous M1 receptors cause only minor PIP_2 breakdown. Furthermore, unlike in our low-level retroviral overexpression studies, in HEK-293 cells TRPM7 overexpression inhibited carbachol-induced PLC signaling (Takezawa et al., 2004). Their study furthermore relied on the use of the 'PLC inhibitor' U-73122, a compound with many known side effects (Balla, 2001; Horowitz et al., 2005). Rather, Takezawa and colleagues suggested that the modulatory effects of carbachol are mediated by cAMP, as lowering $[cAMP]_i$ attenuated whole-cell TRPM7 currents in HEK-293 cells. However, in N1E-115 cells bradykinin had no effect on cAMP levels, and conversely, potent cAMP-raising agonists did not trigger TRPM7 currents or sustained Ca^{2+} influx.

.Superficially, it could be disturbing that perforated-patch currents reported here are relatively small and lack strong outward rectification, a feature that has been termed 'TRPM7 signature'. However, small amplitude basal and evoked currents are to be expected from the experimental conditions used in this study: first, we expressed the channels at low levels and secondly, we detected currents at negative voltages to assess the inward conductance properties and allow comparison with the Ca^{2+} data. TRPM7 inward currents consist mainly of Ca^{2+} and Mg^{2+} ions that both have low permeation rate (Runnels et al., 2001; Nadler et al., 2001) and in HEK-293 overexpression studies inward currents are also minor. Strong outward rectification is seen under conditions of low $[Mg^{2+}]_i$. Interestingly, like the perforated-patch currents, the currents evoked by PLC activation in TRPM7-transfected HEK-293 cells with 1 mM Mg^{2+} in the pipette show only weak outward rectification (Fig. 6*b*). Perhaps this reflects an anomalous mole fraction effect, whereby Mg^{2+}_i attenuates outward monovalent currents. However, separation of this effect from the inhibitory effect of Mg^{2+}_i on channel gating would require systematic analysis (preferably in inside-out patches) that to our knowledge have not been performed thusfar.

In summary, our experiments reveal a second mode of activation for TRPM7: not only can the channel be activated by depletion of intracellular Mg^{2+}, but also by stimulation of endogenous PLC-activating receptors.

Acknowledgements

We thank Dr. T. Balla (NIH, Bethesda, USA), Dr W.J.J.M Scheenen (Radboud University, Nijmegen, NL) and Dr. G. Borst (Erasmus University, Rotterdam, NL) for critical

proofreading of the manuscript. We are also indebted to members of our departments, and to Drs. N. Divecha, J. Halstead and W.H. Moolenaar (Department of Biochemistry, NKI, NL) for stimulating discussions and critical remarks. G. van der Krogt is acknowledged for experimental help. This work was supported by The Dutch Cancer Society.

References

Aarts,M., K.Iihara, W.L.Wei, Z.G.Xiong, M.Arundine, W.Cerwinski, J.F.MacDonald, and M.Tymianski. 2003. A key role for TRPM7 channels in anoxic neuronal death. *Cell* 115:863-877.

Albert,O., N.Ancellin, L.Preisser, A.Morel, and B.Corman. 1999. Serotonin, bradykinin and endothelin signalling in a sheep choroid plexus cell line. *Life Sci.* 64:859-867.

Bacskai,B.J., B.Hochner, M.Mahaut-Smith, S.R.Adams, B.K.Kaang, E.R.Kandel, and R.Y.Tsien. 1993. Spatially resolved dynamics of cAMP and protein kinase A subunits in Aplysia sensory neurons. *Science* 260:222-226.

Balla,T. 2001. Pharmacology of phosphoinositides, regulators of multiple cellular functions. *Curr. Pharm. Des* 7:475-507.

Bolsover,S.R. 1986. Two components of voltage-dependent calcium influx in mouse neuroblastoma cells. Measurement with arsenazo III. *J. Gen. Physiol* 88:149-165.

Clapham,D.E. 2003. TRP channels as cellular sensors. *Nature* 426:517-524.

Clark,K., M.Langeslag, L.B.van, L.Ran, A.G.Ryazanov, C.G.Figdor, W.H.Moolenaar, K.Jalink, and F.N.van Leeuwen. 2006. TRPM7, a novel regulator of actomyosin contractility and cell adhesion. *EMBO J.* 25:290-301.

Coggan,J.S. and S.H.Thompson. 1995. Intracellular calcium signals in response to bradykinin in individual neuroblastoma cells. *Am. J. Physiol* 269:C841-C848.

Demeuse,P., R.Penner, and A.Fleig. 2006. TRPM7 Channel Is Regulated by Magnesium Nucleotides via its Kinase Domain. *J. Gen. Physiol* 127:421-434.

Grynkiewicz,G., M.Poenie, and R.Y.Tsien. 1985. A new generation of Ca2+ indicators with greatly improved fluorescence properties. *J. Biol. Chem.* 260:3440-3450.

Hanano,T., Y.Hara, J.Shi, H.Morita, C.Umebayashi, E.Mori, H.Sumimoto, Y.Ito, Y.Mori, and R.Inoue. 2004. Involvement of TRPM7 in cell growth as a spontaneously activated Ca2+ entry pathway in human retinoblastoma cells. *J. Pharmacol. Sci.* 95:403-419.

Hanke,S., B.Nurnberg, D.H.Groll, and C.Liebmann. 2001. Cross talk between beta-adrenergic and bradykinin B(2) receptors results in cooperative regulation of cyclic AMP accumulation and mitogen-activated protein kinase activity. *Mol. Cell Biol.* 21:8452-8460.

Hermosura,M.C., M.K.Monteilh-Zoller, A.M.Scharenberg, R.Penner, and A.Fleig. 2002. Dissociation of the store-operated calcium current I(CRAC) and the Mg-nucleotide-regulated metal ion current MagNuM. *J. Physiol* 539:445-458.

Honda,A., S.R.Adams, C.L.Sawyer, V.Lev-Ram, R.Y.Tsien, and W.R.Dostmann. 2001. Spatiotemporal dynamics of guanosine 3',5'-cyclic monophosphate revealed by a genetically encoded, fluorescent indicator. *Proc. Natl. Acad. Sci. U. S. A* 98:2437-2442.

Horowitz,L.F., W.Hirdes, B.C.Suh, D.W.Hilgemann, K.Mackie, and B.Hille. 2005. Phospholipase C in living cells: activation, inhibition, Ca2+ requirement, and regulation of M current. *J. Gen. Physiol* 126:243-262.

Hoth,M. and R.Penner. 1992. Depletion of intracellular calcium stores activates a calcium current in mast cells. *Nature* 355:353-356.

Jalink,K., E.J.van Corven, and W.H.Moolenaar. 1990. Lysophosphatidic acid, but not phosphatidic acid, is a potent Ca2(+)-mobilizing stimulus for fibroblasts. Evidence for an extracellular site of action. *J. Biol. Chem.* 265:12232-12239.

Jiang,X., E.W.Newell, and L.C.Schlichter. 2003. Regulation of a TRPM7-like current in rat brain microglia. *J. Biol. Chem.* 278:42867-42876.

Kerschbaum,H.H., J.A.Kozak, and M.D.Cahalan. 2003. Polyvalent cations as permeant probes of MIC and TRPM7 pores. *Biophys. J.* 84:2293-2305.

Kim,B.J., H.H.Lim, D.K.Yang, J.Y.Jun, I.Y.Chang, C.S.Park, I.So, P.R.Stanfield, and K.W.Kim. 2005. Melastatin-type transient receptor potential channel 7 is required for intestinal pacemaking activity. *Gastroenterology* 129:1504-1517.

Kozak,J.A. and M.D.Cahalan. 2003. MIC channels are inhibited by internal divalent cations but not ATP. *Biophys. J.* 84:922-927.

Kozak,J.A., H.H.Kerschbaum, and M.D.Cahalan. 2002. Distinct properties of CRAC and MIC channels in RBL cells. *J. Gen. Physiol* 120:221-235.

Lepple-Wienhues,A. and M.D.Cahalan. 1996. Conductance and permeation of monovalent cations through depletion-activated Ca2+ channels (ICRAC) in Jurkat T cells. *Biophys. J.* 71:787-794.

Ling,L.E., J.T.Schulz, and L.C.Cantley. 1989. Characterization and purification of membrane-associated phosphatidylinositol-4-phosphate kinase from human red blood cells. *J. Biol. Chem.* 264:5080-5088.

Liu,B. and F.Qin. 2005. Functional control of cold- and menthol-sensitive TRPM8 ion channels by phosphatidylinositol 4,5-bisphosphate. *J. Neurosci.* 25:1674-1681.

Liu,D. and E.R.Liman. 2003. Intracellular Ca2+ and the phospholipid PIP2 regulate the taste transduction

ion channel TRPM5. *Proc. Natl. Acad. Sci. U. S. A* 100:15160-15165.

Matsushita,M., J.A.Kozak, Y.Shimizu, D.T.McLachlin, H.Yamaguchi, F.Y.Wei, K.Tomizawa, H.Matsui, B.T.Chait, M.D.Cahalan, and A.C.Nairn. 2005. Channel function is dissociated from the intrinsic kinase activity and autophosphorylation of TRPM7/ChaK1. *J. Biol. Chem.* 280:20793-20803.

Mau,S.E., P.J.Larsen, J.A.Mikkelsen, and T.Saermark. 1990. Substance P and related tachykinins induce receptor-mediated hydrolysis of polyphosphoinositides in the rat anterior pituitary. *Mol. Cell Endocrinol.* 69:69-78.

Miyawaki,A., J.Llopis, R.Heim, J.M.McCaffery, J.A.Adams, M.Ikura, and R.Y.Tsien. 1997. Fluorescent indicators for Ca2+ based on green fluorescent proteins and calmodulin. *Nature* 388:882-887.

Monteilh-Zoller,M.K., M.C.Hermosura, M.J.Nadler, A.M.Scharenberg, R.Penner, and A.Fleig. 2003. TRPM7 provides an ion channel mechanism for cellular entry of trace metal ions. *J. Gen. Physiol* 121:49-60.

Nadler,M.J., M.C.Hermosura, K.Inabe, A.L.Perraud, Q.Zhu, A.J.Stokes, T.Kurosaki, J.P.Kinet, R.Penner, A.M.Scharenberg, and A.Fleig. 2001. LTRPC7 is a Mg.ATP-regulated divalent cation channel required for cell viability. *Nature* 411:590-595.

Perraud,A.L., A.Fleig, C.A.Dunn, L.A.Bagley, P.Launay, C.Schmitz, A.J.Stokes, Q.Zhu, M.J.Bessman, R.Penner, J.P.Kinet, and A.M.Scharenberg. 2001. ADP-ribose gating of the calcium-permeable LTRPC2 channel revealed by Nudix motif homology. *Nature* 411:595-599.

Ponsioen,B., J.Zhao, J.Riedl, F.Zwartkruis, K.G.van der, M.Zaccolo, W.H.Moolenaar, J.L.Bos, and K.Jalink. 2004. Detecting cAMP-induced Epac activation by fluorescence resonance energy transfer: Epac as a novel cAMP indicator. *EMBO Rep.* 5:1176-1180.

Postma,F.R., K.Jalink, T.Hengeveld, A.G.Bot, J.Alblas, H.R.de Jonge, and W.H.Moolenaar. 1996a. Serum-induced membrane depolarization in quiescent fibroblasts: activation of a chloride conductance through the G protein-coupled LPA receptor. *EMBO J.* 15:63-72.

Postma,F.R., K.Jalink, T.Hengeveld, and W.H.Moolenaar. 1996b. Sphingosine-1-phosphate rapidly induces Rho-dependent neurite retraction: action through a specific cell surface receptor. *EMBO J.* 15:2388-2392.

Prakriya,M. and R.S.Lewis. 2002. Separation and characterization of currents through store-operated CRAC channels and Mg2+-inhibited cation (MIC) channels. *J. Gen. Physiol* 119:487-507.

Prescott,E.D. and D.Julius. 2003. A modular PIP2 binding site as a determinant of capsaicin receptor sensitivity. *Science* 300:1284-1288.

Rae,J., K.Cooper, P.Gates, and M.Watsky. 1991. Low access resistance perforated patch recordings using amphotericin B. *J. Neurosci. Methods* 37:15-26.

Rohacs,T., C.M.Lopes, I.Michailidis, and D.E.Logothetis. 2005. PI(4,5)P2 regulates the activation and desensitization of TRPM8 channels through the TRP domain. *Nat. Neurosci.* 8:626-634.

Runnels,L.W., L.Yue, and D.E.Clapham. 2002. The TRPM7 channel is inactivated by PIP(2) hydrolysis. *Nat. Cell Biol.* 4:329-336.

Runnels,L.W., L.Yue, and D.E.Clapham. 2001. TRP-PLIK, a bifunctional protein with kinase and ion channel activities. *Science* 291:1043-1047.

Schmitz,C., M.V.Dorovkov, X.Zhao, B.J.Davenport, A.G.Ryazanov, and A.L.Perraud. 2005. The channel kinases TRPM6 and TRPM7 are functionally nonredundant. *J. Biol. Chem.* 280:37763-37771.

Schmitz,C., A.L.Perraud, C.O.Johnson, K.Inabe, M.K.Smith, R.Penner, T.Kurosaki, A.Fleig, and A.M.Scharenberg. 2003. Regulation of vertebrate cellular Mg2+ homeostasis by TRPM7. *Cell* 114:191-200.

Su,L.T., M.A.Agapito, M.Li, T.N.Simonson, A.Huttenlocher, R.Habas, L.Yue, and L.W.Runnels. 2006. Trpm7 regulates cell adhesion by controlling the calcium dependent protease calpain. *J. Biol. Chem.*

Takezawa,R., C.Schmitz, P.Demeuse, A.M.Scharenberg, R.Penner, and A.Fleig. 2004. Receptor-mediated regulation of the TRPM7 channel through its endogenous protein kinase domain. *Proc. Natl. Acad. Sci. U. S. A* 101:6009-6014.

van der Wal,W.J., R.Habets, P.Varnai, T.Balla, and K.Jalink. 2001. Monitoring agonist-induced phospholipase C activation in live cells by fluorescence resonance energy transfer. *J. Biol. Chem.* 276:15337-15344.

Voets,T., B.Nilius, S.Hoefs, A.W.van der Kemp, G.Droogmans, R.J.Bindels, and J.G.Hoenderop. 2004. TRPM6 forms the Mg2+ influx channel involved in intestinal and renal Mg2+ absorption. *J. Biol. Chem.* 279:19-25.

Xu,C., J.Watras, and L.M.Loew. 2003. Kinetic analysis of receptor-activated phosphoinositide turnover. *J. Cell Biol.* 161:779-791.

Zaccolo,M., G.F.De, C.Y.Cho, L.Feng, T.Knapp, P.A.Negulescu, S.S.Taylor, R.Y.Tsien, and T.Pozzan. 2000. A genetically encoded, fluorescent indicator for cyclic AMP in living cells. *Nat. Cell Biol.* 2:25-29.

Zweifach,A. and R.S.Lewis. 1993. Mitogen-regulated Ca2+ current of T lymphocytes is activated by depletion of intracellular Ca2+ stores. *Proc. Natl. Acad. Sci. U. S. A* 90:6295-6299.